

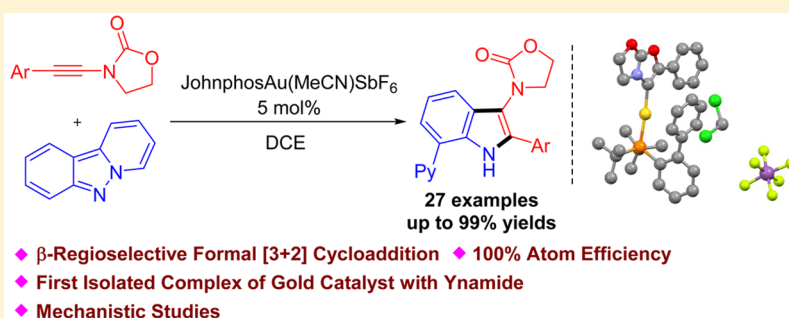
Gold-Catalyzed β -Regioselective Formal [3 + 2] Cycloaddition of Ynamides with Pyrido[1,2-*b*]indazoles: Reaction Development and Mechanistic Insights

Yinghua Yu,^{†,§} Gui Chen,^{†,§} Lei Zhu,[†] Yun Liao,^{†,‡} Yufeng Wu,^{†,‡} and Xueliang Huang^{*,†}

[†]Key Laboratory of Coal to Ethylene Glycol and Its Related Technology, Fujian Institute of Research on the Structure of Matter, Chinese Academy of Sciences, Yangqiao West Road 155#, Fuzhou, Fujian 350002, China

[‡]College of Chemistry, Fuzhou University, Fuzhou, Fujian 350108, China

S Supporting Information



ABSTRACT: Here, we report an unprecedented gold(I)-induced β -site regioselective formal [3 + 2] cycloaddition of ynamides with pyrido[1,2-*b*]indazoles, giving 3-amido-7-(pyrid-2'-yl)indoles in good to excellent yields. A complex of gold(I) catalyst with ynamide was isolated and characterized by X-ray diffraction analysis for the first time. Mechanistic investigations suggest the reaction pathway involves a gold-stabilized carbocation intermediate, which in turn participated in sequential C–H bond functionalization of the *ortho*-position of the phenyl ring.

INTRODUCTION

Ynamides are bench stable and easily accessible starting materials. In the past decade, a large library of nitrogen-containing molecules have been prepared via addition of nucleophiles to the α -site of ynamides (Scheme 1a).^{1,2} In contrast, the addition of nucleophiles at the β position of the triple bond is comparatively less common.^{3,4} Very recently, Marek,^{3a} Lam,^{3c} and others^{3d,e} reported carbometalation of ynamides in the presence of proper copper(I) or rhodium(I) salts, in which the tethered carbamate functionality was crucial for the β -regioselectivity by acting as a chelating group. Herein, we report the first gold-catalyzed β -regioselective cycloaddition of ynamides with external reagents, giving 3-amidoindole derivatives in an atom-economical manner (Scheme 1b). Hashmi^{4a} and Gagosz^{4b} have reported gold-catalyzed intramolecular cyclization of *N*-alkynyl *tert*-butyloxycarbamates independently. However, to our knowledge, gold-catalyzed intermolecular cycloaddition of ynamides with other reactants featuring β -regioselectivity has remained elusive to date.

Gold-catalyzed reactions of alkynes with nucleophiles have received considerable attention.⁵ Compared with the relatively well investigated approach to generate α -carbonyl gold-carbene,⁶ a similar but equally appealing concept on gold-catalyzed formation of α -imino carbene remains underdeveloped.⁷ Seminal works on gold-catalyzed nitrene transfer

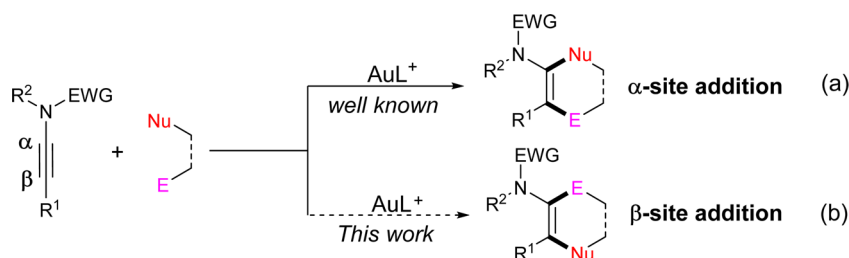
by intramolecular reaction of alkynyl azides were first described by Toste in 2005⁸ and further demonstrated by Zhang,⁹ Gagosz,¹⁰ and others.¹¹ Instead of azides, anthranils and other nitrene-transfer reagents have been used as nitrene precursors.¹² Intermolecular reactions of azides with ynamides have also been realized by Ye,¹³ Liu,¹⁴ and our group^{15a,b} very recently. In conjunction with our continuing interest in nitrogen-containing molecule synthesis via α -imino carbene intermediates,¹⁵ we envisioned that gold-catalyzed reaction of ynamide **1a** with azide **b** might generate intermediate **B**, which in turn will undergo intramolecular cyclization with a tethered pyridinyl moiety, eventually leading to the formation of fused tricyclic compound **1ab** (Scheme 2).

Herein, we present our detailed studies toward this goal and disclose an unprecedented gold-catalyzed annulation of ynamides with pyrido[1,2-*b*]indazoles, providing 3-amino-7-(pyrid-2'-yl)indoles in good to excellent yields. The regioselectivity of the current transformation suggests an unusual β -site cycloaddition of ynamide was involved. A series of mechanistic studies were performed to get valuable information on the reaction pathways. Moreover, a complex of gold catalyst

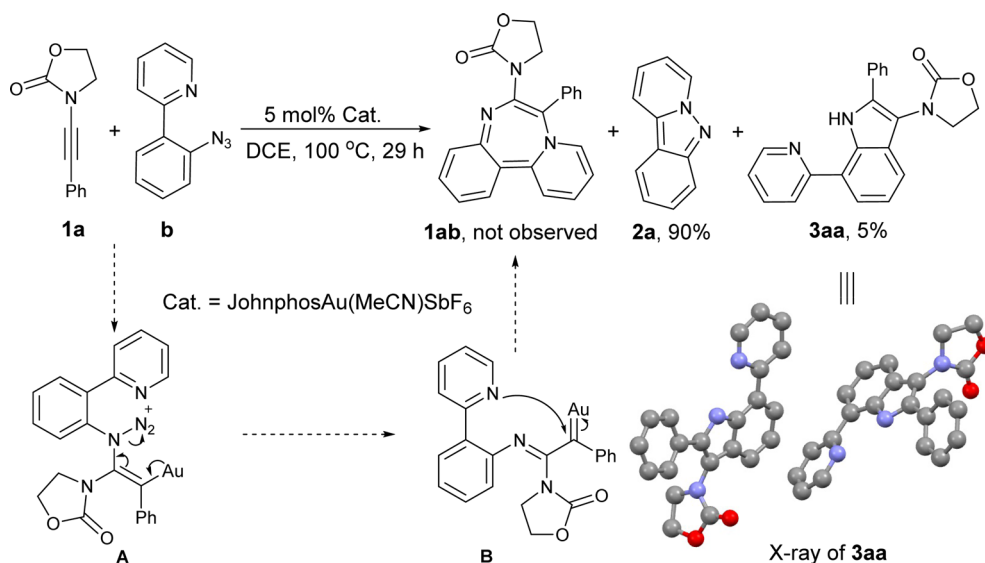
Received: August 8, 2016

Published: August 28, 2016

Scheme 1. Gold-Catalyzed Formal Cycloaddition of Ynamides



Scheme 2. Initial Attempts toward Original Hypothesis



with ynamide was isolated for the first time and characterized by single-crystal X-ray analysis.

RESULTS AND DISCUSSION

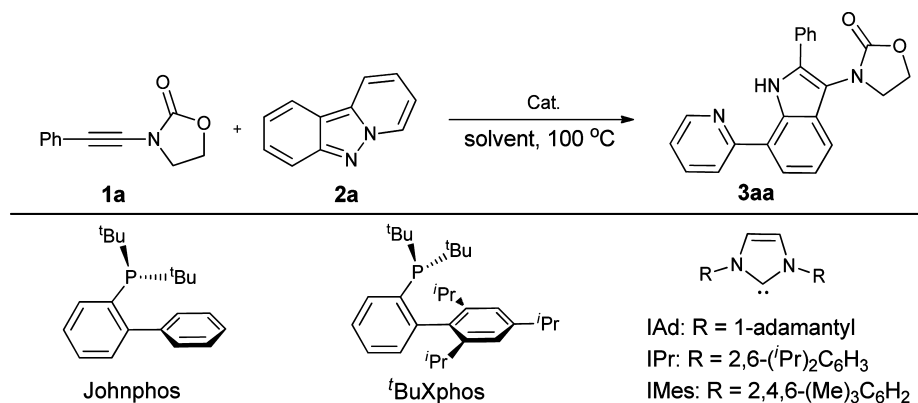
Optimization Studies and Substrate Scope. To test our hypothesis, the reaction of ynamide **1a** and 2-(2-azidophenyl)pyridine (**b**) was evaluated initially (Scheme 2). Using $\text{JohnphosAu}(\text{MeCN})\text{SbF}_6$ (Echavarren's catalyst, 5 mol %) as catalyst,¹⁶ azide **b** was completely consumed after heating at 100 °C for 29 h in DCE (1,2-dichloroethane), while most ynamide **1a** remained intact, and the suspecting product **1ab** was not observed from the reaction mixture. Pyrido[1,2-*b*]indazole (**2a**) was obtained as the major product, which was presumably resulting from the ring closure of **b** by thermolysis.¹⁷ Surprisingly, a new compound which was identified as 3-amino-7-(pyrid-2'-yl)indole (**3aa**)¹⁸ was obtained in 5% yield upon isolation. Unambiguous proof of structure and regioselectivity was achieved by single-crystal X-ray analysis. Pleasingly, under otherwise identical conditions but replacing **b** with pyrido[1,2-*b*]indazole (**2a**), **3aa** was obtained as the sole product in nearly quantitative yield. It is worth mentioning that Hashmi^{12a} and Ye^{12c} reported elegant gold-catalyzed annulations of anthranils or isoxazoles with ynamides to synthesize polysubstituted pyrroles or 7-acylindoles very recently. In their report, α -site regiocontrolled addition of ynamides occurred exclusively. In contrast, the precise structure of **3aa** suggests an unusual β -site addition of ynamide **1a** takes place here. This observation indicates that a key reaction intermediate distinct from well-accepted keteni-

mium ion was involved in this novel transformation (vide infra).

As one of the most important classes of heterocycles, indole scaffolds are embedded in a wide range of natural products and pharmaceuticals.¹⁹ Therefore, the development of efficient methodologies to access these compounds has received long-term attention.²⁰ Compared with a normal indole moiety, the classic Fisher cyclization is not applicable to preparation of 7-(pyrid-2'-yl)indoles.²¹ Moreover, regarding their potential utilities in pharmaceuticals and material science,^{21b,22,23} and the abnormal β -regioselective addition of the ynamides in current transformation, we decided to explore the reaction of ynamides with pyrido[1,2-*b*]indazole systematically.

As depicted in Table 1, a series of gold catalysts containing different counteranions and ligands were examined. JohnphosAuNTf_2 was found to be less reactive (entry 2). Other cationic catalysts bearing simple phosphine or N-heterocyclic carbene ligands including $\text{PPh}_3\text{AuNTf}_2$, $\text{IAdAu}(\text{PhCN})\text{SbF}_6$, and IPrAuNTf_2 were proven to be less efficient or totally inactive (entries 4–8). AgSbF_6 or HOTf showed no catalytic activity for the reaction (entries 9 and 10). The effects of solvent were also examined (entries 11–15). CH_2Cl_2 , toluene, and CHCl_3 were proper reaction media, while low yields of indole **3aa** were observed when the reactions were performed in MeNO_2 or MeCN .

With a set of efficient reaction conditions established (Table 1, entry 1), the reaction scope was explored by using pyrido[1,2-*b*]indazole (**2a**) as the nitrene precursor. The results are shown in Table 2. In general, both electron-donating (methyl, ethyl, and methoxyl, cf. **3ba–da**) and electron-

Table 1. Optimization of the Reaction Conditions^a

entry	cat.	solvent	time (h)	yield ^b (%)
1	JohnPhosAu(MeCN)SbF ₆	DCE	11	96 (95) ^c
2	JohnPhosAuNTf ₂	DCE	16	88
3	JohnPhosAuCl	DCE	16	
4	PPh ₃ AuNTf ₂	DCE	16	31
5	^t BuXPhosAu(MeCN)SbF ₆	DCE	22	8
6	IAdAu(PhCN)SbF ₆	DCE	16	12
7	IPrAuNTf ₂	DCE	16	
8	IMesAuSbF ₆	DCE	16	
9	AgSbF ₆	DCE	16	
10	HOTf	DCE	16	
11	JohnPhosAu(MeCN)SbF ₆	DCM	16	85
12	JohnPhosAu(MeCN)SbF ₆	toluene	16	86
13	JohnPhosAu(MeCN)SbF ₆	CHCl ₃	16	83
14	JohnPhosAu(MeCN)SbF ₆	MeNO ₂	16	66
15	JohnPhosAu(MeCN)SbF ₆	MeCN	16	71

^a **1a** (0.2 mmol), **2a** (0.24 mmol), and 5 mol % of catalysts were stirred in solvent (1 mL) at 100 °C for the proper reaction time. ^b Determined by ¹H NMR using CH₂Br₂ as internal standard. ^c Yield given within parentheses refers to the pure product.

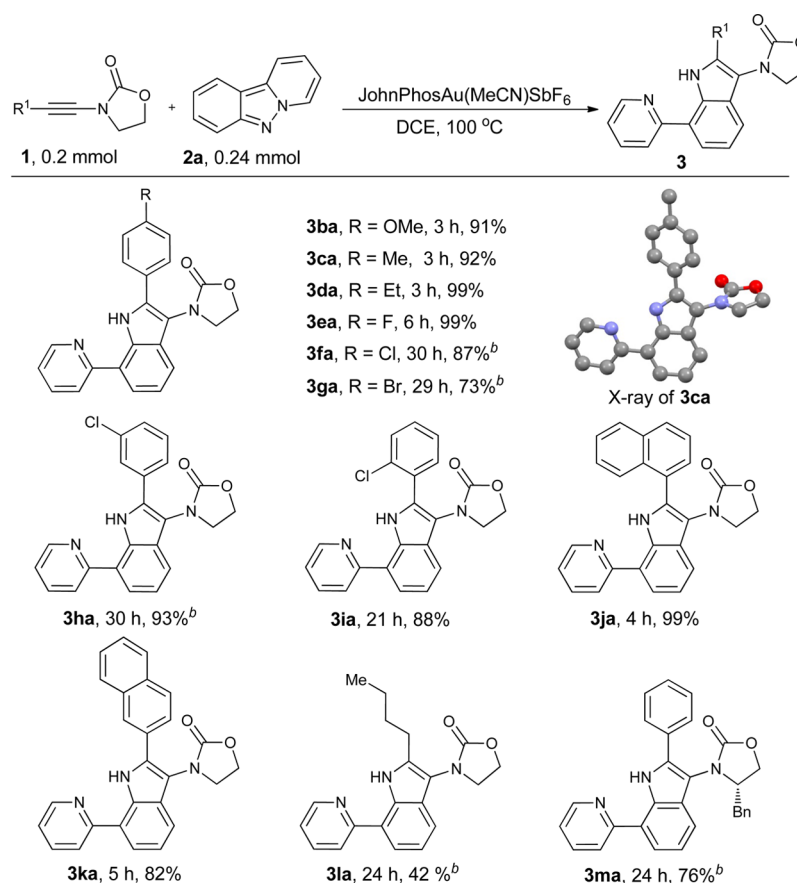
withdrawing groups (fluoro, chloro and bromo, cf. **3ea–ia**) on the phenyl ring of ynamides **1** were tolerated, furnishing the corresponding indoles in good to excellent yields. Moreover, ynamides bearing 1-naphthyl or 2-naphthyl at the terminal position of the triple bond were viable substrates. Compounds **3ja** and **3ka** were obtained in 99% and 82% yield, respectively. Ynamide (**1l**), derived from hex-1-yne, could participate in the reaction, albeit with 42% yield (cf. **3la**). The reaction of ynamide **1m** bearing a chiral auxiliary group proceeded well, furnishing indole **3ma** in 76% yield. Given the abundance and the easy accessibility of chiral oxazolidin-2-ones, such kinds of 7-(pyrid-2'-yl)indoles may have synthetic potential in the area of chiral bidentated anion ligands.

Subsequently, the generality and limitation of pyrido[1,2-*b*]indazoles for the reaction with ynamide **1a** was investigated under the standard reaction conditions. As depicted in Table 3, a broad set of substituents on pyrido[1,2-*b*]indazole were proven to be compatible (**3ab–ap**). Notably, electron-withdrawing groups (R²) trended to speed up the reaction and afford the corresponding products in higher yields (Table 3 and Scheme S1).

Mechanistic Studies: Detection and Characterization of Reaction Intermediates. The unusual regioselectivity of gold-catalyzed annulation between ynamides and pyrido[1,2-*b*]indazoles is intriguing. To gain a deeper understanding on the reaction mechanism, a series of experiments were subsequently conducted. The stoichiometric reactions of **1a** and **2a** with catalyst JohnphosAu(MeCN)SbF₆ were monitored

by ³¹P NMR spectroscopy in CDCl₃ at room temperature (Figure 1 and Figure S1). Treatment of **1a** with JohnphosAu(MeCN)SbF₆ generated a new species with ³¹P NMR shift at 64.28 ppm (Figure 1c), which has been identified as the adduct of **1a** with the cationic gold catalyst. The structure of this complex was confirmed by X-ray crystallography,²⁴ which contained a fused bicyclic five-membered-ring system (Figure 2). Compared with the extensive studies on gold-catalyzed formal cycloaddition of ynamides in recent years, the current outcome is noteworthy. The well-accepted keteniminium ion intermediate, which would commonly lead to an α -site-selective cycloaddition product, was not observed. More importantly, in previous reports, the activation mode of gold catalyst with ynamide is somewhat speculative. No direct evidence for the actual reaction intermediate has been described. The adduct obtained here represents the first isolated gold complex with ynamide, and it well explained the unusual β -site regioselective addition observed in the current transformation. Encouraged by this discovery, further systematic examinations on the complexation of gold catalysts with other ynamides will be the subject of future studies.

On the other hand, the reaction of **2a** with JohnphosAu(MeCN)SbF₆ gave JohnphosAu(**2a**)SbF₆. The structure of this complex was also confirmed by X-ray crystallography (Figure 3), and the corresponding ³¹P NMR showed a chemical shift at 59.03 ppm (Figure 1b). Interestingly, upon addition of **2a** to the mixture of JohnphosAu(MeCN)SbF₆ and **1a**, the peak for JohnphosAu(**1a**)SbF₆ disappeared with concomitant formation

Table 2. Reaction Scope of Ynamides^a

^aAll reactions were carried out on a 0.2 mmol scale with 5 mol % of JohnphosAu(MeCN)SbF₆ as catalyst at 100 °C in DCE, [1] = 0.1 M. ^b10 mol % of catalyst was employed.

of a new species, showing a chemical shift at 64.63 ppm (Figure 1d). Although attempts to crystallize the corresponding three-component adduct were not successful, a new species was detected by high-resolution mass spectrometry (HR-MS, *m/z* 850.2901, Figure S2), which could be assigned to a complex of gold catalyst with **1a** and **2a**, namely JohnphosAu(**1a**)(**2a**)SbF₆.

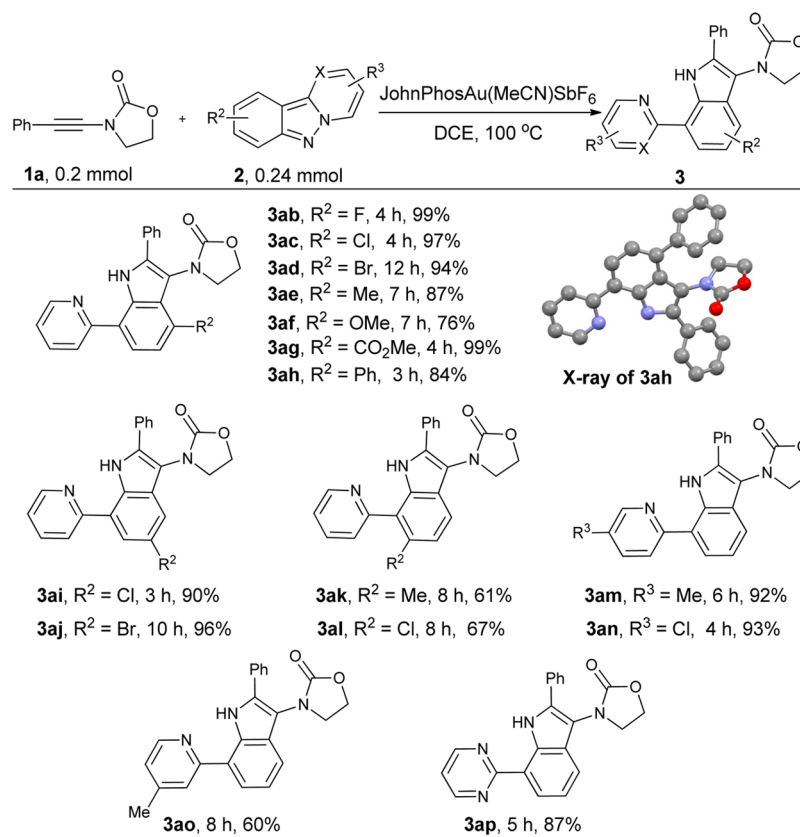
Kinetic studies for the gold-catalyzed reaction of **1a** and **2a** were further carried out to get better understanding of the reaction mechanism. The reaction was found to be first order in JohnphosAu(MeCN)SbF₆ (Figure 4 and Figure S3) and zero-order in both **1a** and **2a** (Figures S4 and S5). Increasing the concentration of **2a** slightly depressed reaction rates, suggesting that **2a** may partially poison the gold catalyst. When the temperature was varied from 313 to 335 K (Figure 5 and Figure S6), activation parameters $\Delta H^\ddagger = 16.8 \text{ kcal mol}^{-1}$ and $\Delta S^\ddagger = -19.1 \text{ cal mol}^{-1} \text{ K}^{-1}$ were obtained from Eyring plots. The negative ΔS^\ddagger value is consistent with our NMR experiments. Kinetics for the reactions of various *para*-substituted ynamides **1** with **2a** were also carried out. A fairly linear Hammett correlation between $\log(k_X/k_H)$ and σ was obtained with a reaction constant of $\rho = -2.15$ (Figure 6 and Figure S7). The large negative ρ value suggests that the transition state of the reaction is polarized with positive charge at the reaction center.

C–H bond functionalization of the aromatic ring was involved in current transformation. To identify whether cleavage of the C–H bond at the *ortho*-position of pyrido[1,2-*b*]indazoles **2a** is involved as the rate-determining step, kinetic isotope effect studies of parallel experiments were

carried out (Scheme 3 and Figure 7). As depicted, no significant kinetic isotope effect ($k_H/k_D = 1.07$) was observed, suggesting that C–H bond cleavage was not involved in the rate-determining step.

Collectively, plausible mechanistic rationales for current indole synthesis were outlined in Scheme 4. Coordination of ynamide **1a** to the gold catalyst **C** would generate intermediate **E** bearing a transient five-membered ring. A nucleophilic attack of **E** by **2a** gave **F**. Ring opening of the pyrido[1,2-*b*]indazole (*b* ring) led to the formation of intermediate **G**. Intramolecular *sp*² C–H bond functionalization (**G** → **H**), followed by protodeauration and isomerization, would furnish the final product 3-aminindole **3aa**. Since enhanced reaction rate and efficiency were observed by setting up electron-withdrawing groups onto a ring (Table 3 and Scheme S1),²⁵ pathways akin to Friedel–Crafts-type alkylation or C–H bond insertion of gold carbene intermediate were unlikely.

During the testing of the scope of ynamides, we found that the reaction of ynamides bearing a sulfonyl protecting group on the nitrogen atom led to no formation of the corresponding 3-amidoindoles (results not shown). Notably, when ynamide **4**, possessing a Cbz (benzyl carbamate) protected amide moiety, was employed instead of **1a**, the target indole was not obtained either (Scheme 5). These observations further highlight the critical role of the oxazolidin-2-onyl moiety for current β -regioselective formal cycloaddition.

Table 3. Reaction Scope of Pyrido[1,2-*b*]indazole^a

^aAll reactions were carried out on a 0.2 mmol scale with 5 mol % of JohnphosAu(MeCN)SbF₆ as catalyst at 100 °C in DCE, [**1a**] = 0.1 M.

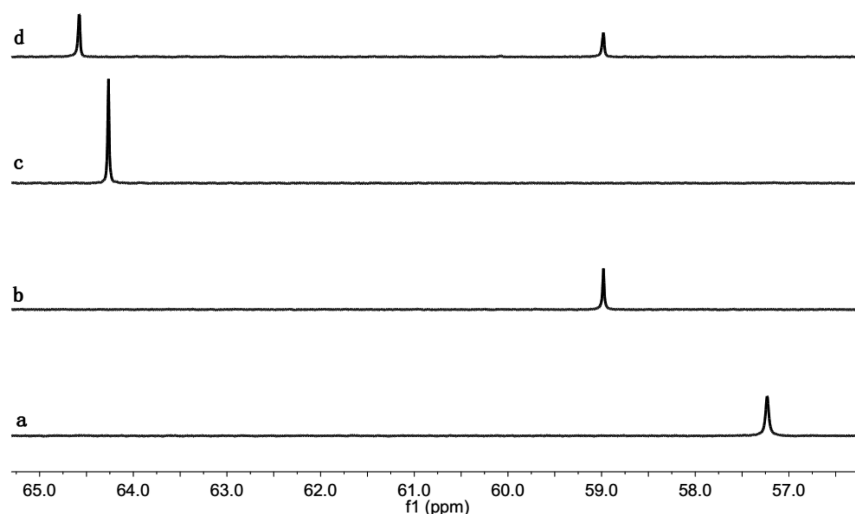


Figure 1. ³¹P NMR spectroscopy of (a) 10 mmol of JohnphosAu(MeCN)SbF₆, (b) mixture of 10 mmol of JohnphosAu(MeCN)SbF₆ and 10 mmol of **2a**, (c) mixture of 10 mmol of JohnphosAu(MeCN)SbF₆ and 20 mmol of **1a**, and (d) mixture of 10 mmol of JohnphosAu(MeCN)SbF₆, 20 mmol of **1a**, and 20 mmol of **2a** in 0.5 mL of CDCl₃.

CONCLUSIONS

In summary, we have demonstrated a novel gold-catalyzed formal [3 + 2] cycloaddition of ynamides with pyrido[1,2-*b*]indazoles, furnishing 3-amido-7-(pyrid-2'-yl)indoles in good to excellent yields. Compared with previous relatively extensive studies on gold-catalyzed reactions of ynamides, the current transformation has showcased an unusual β -site-regioselective formal cycloaddition of pyrido[1,2-*b*]indazoles **2** to ynamides **1**,

thus leading 3-amidoindoles exclusively. According to this activation mode, we believe that a number of new reactions that feature β -site regioselective addition of ynamides will be uncovered in the near future.

EXPERIMENTAL SECTION

General Information. JohnphosAu(MeCN)SbF₆,¹⁶ ynamides **1**,²⁶ and pyrido[1,2-*b*]indazoles **2**¹⁷ were prepared according to literature methods. All reactions were carried out with standard Schlenk

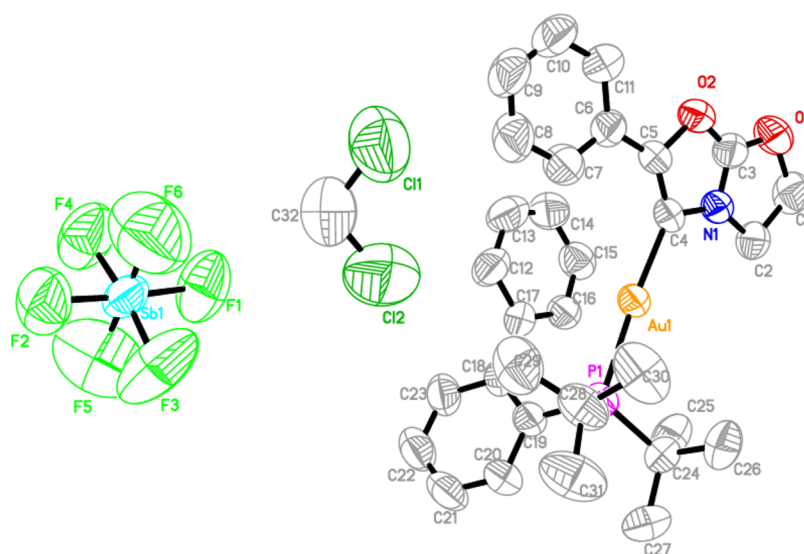


Figure 2. X-ray structure of JohnphosAu(1a)SbF₆. Hydrogen atoms have been omitted for clarity.

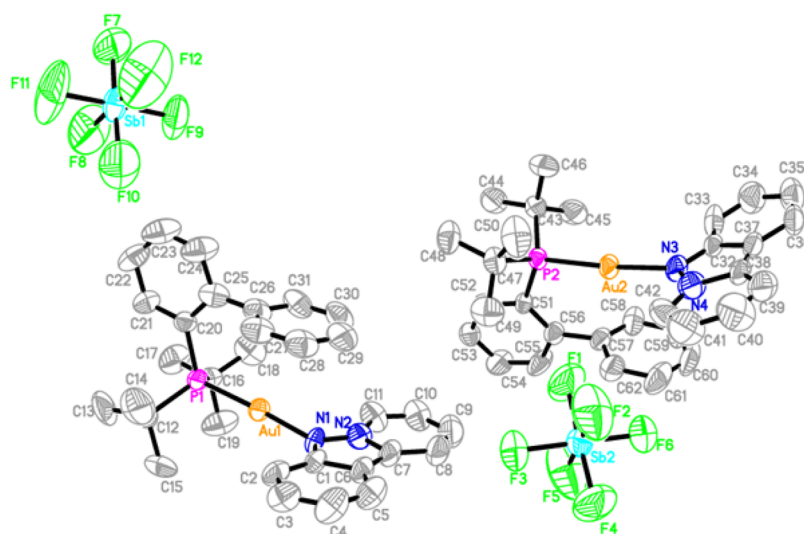


Figure 3. X-ray structure of JohnphosAu(2a)SbF₆. Hydrogen atoms have been omitted for clarity.

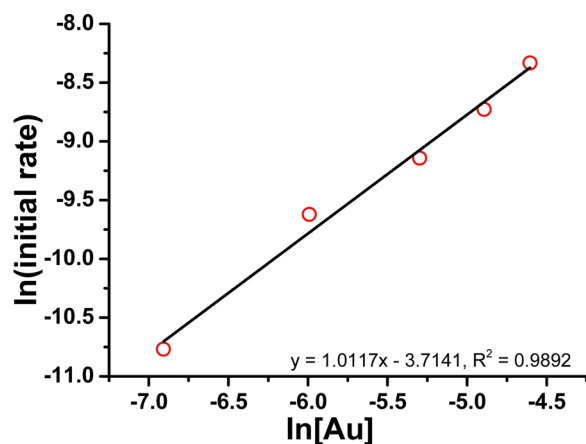


Figure 4. Plot of $\ln(\text{initial rate})$ vs $\ln[\text{Au}]$. $y = 1.0117x - 3.7141$, $R^2 = 0.9892$. The slope of the line is approximately 1, indicating that the rate for the reaction is first order in JohnphosAu(MeCN)SbF₆.

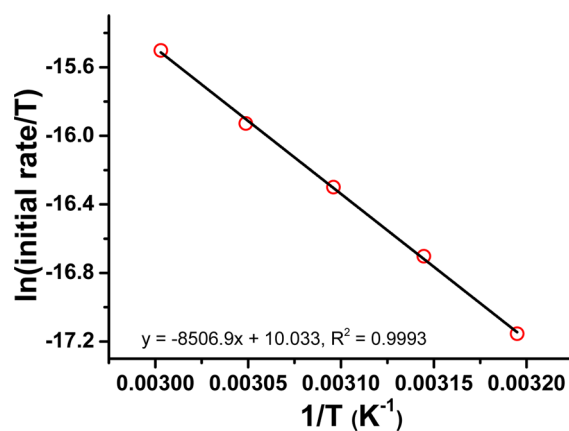


Figure 5. Plot of $\ln(\text{initial rate}/T)$ vs $1/T$ for the reaction between **1a** and **2a** in CDCl₃, $[\mathbf{1a}] = 0.10$ M, $[\mathbf{2a}] = 60$ mM, $[\text{Au}] = 2.5$ mM. Slope = -8.51×10^3 , y -intercept = 1.00×10 , $R^2 = 0.999$.

techniques under argon. All reagents were used as received from commercial suppliers unless otherwise stated. All solvents were

purified by distillation following standard procedures. Reaction progress was monitored by thin-layer chromatography (TLC), and

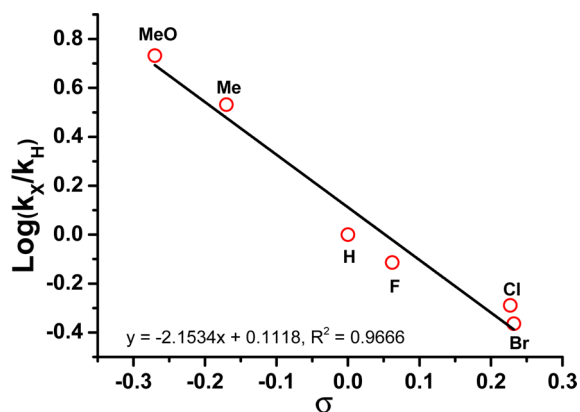


Figure 6. Hammett plot of $\log(k_X/k_H)$ vs σ for the reaction of **2a** with *para*-substituted ynamides **1** in CDCl_3 at 60°C , $[\mathbf{1a}] = 0.10\text{ M}$, $[\mathbf{2a}] = 60\text{ mM}$, $[\text{Au}] = 2.5\text{ mM}$. Slope = -2.15 , y -intercept = 0.11 , $R^2 = 0.967$.

components were visualized by observation under UV light at 254 nm. Flash column chromatography was performed using silica gel 60 (200–300 mesh). High-resolution mass spectrometry was performed on a UHR TOF LC/MS mass spectrometer. All ^1H , ^{13}C , and ^{31}P NMR spectra were recorded on a 400 MHz spectrometer (^1H 400 MHz, ^{13}C 100 MHz, ^{31}P 162 MHz) using CDCl_3 as solvent. Chemical shifts were reported in parts per million (ppm, δ). ^1H NMR spectra are referenced to the peak of tetramethylsilane ($\delta = 0.00$) and reported as follows: chemical shift (ppm), multiplicity (s = singlet, t = triplet, q = quartet, m = multiplet), and coupling constant (Hz). ^{13}C NMR spectra are referenced to the solvent center peak of CDCl_3 ($\delta = 77.0$). ^{31}P NMR spectra are referenced to the peak of H_3PO_4 ($\delta = 0.00$). Crystallographic data are available.²⁷

Synthesis of Pyrido[1,2-*b*]indazole **2.** A solution of 2-phenylpyridine (2 mmol), $[\text{Cp}^*\text{RhCl}_2]_2$ (4 mol %), $\text{PhI}(\text{OAc})_2$ (1.5 equiv), and *p*-TsOH· H_2O (1.5 equiv) in 15 mL of acetone was stirred at room temperature for 15 min. After addition of NaN_3 (6 mmol), the reaction mixture was stirred at 50°C for 16 h. Then the solvent was removed under reduced pressure, and the residue was purified by silica gel chromatography using EA/PE as eluent to afford the azidation product 2-(2-azidophenyl)pyridine (**b**) in 88% yield. 2-(2-Azidophenyl)pyridine (**b**) and dry dioxane (5 mL) were charged into a pressure tube under nitrogen. After the mixture was stirred at 125°C for 8–20 h, the solvent was removed on a rotary evaporator and the residue was purified by column chromatography on silica gel (ethyl acetate/petroleum ether = 10:1) to afford the product pyrido[1,2-*b*]indazole (**2a**).

^1H and ^{13}C NMR Spectral Data for the Prepared Substrates. 2-(2-Azidophenyl)pyridine (**b**): ^1H NMR (400 MHz, CDCl_3) δ 8.71 (d, $J = 4.4\text{ Hz}$, 1H), 7.74–7.65 (m, 3H), 7.43 (t, $J = 7.2\text{ Hz}$, 1H),

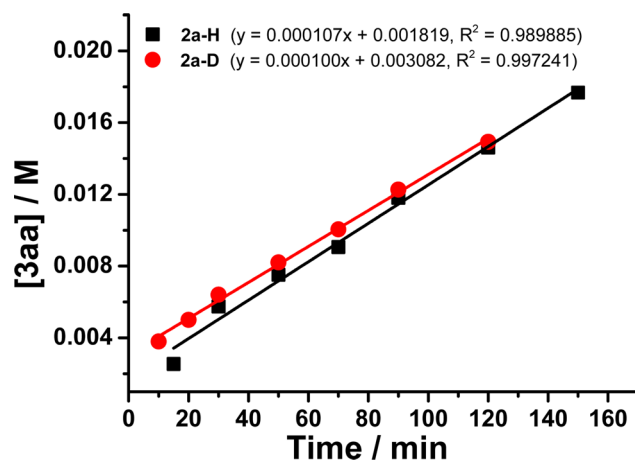


Figure 7. Kinetic profiles for the gold-catalyzed annulation of ynamides **1a** with pyrido[1,2-*b*]indazoles **2a-H** (black) and **2a-D** (red). Yields were obtained by ^1H NMR using dibromomethane as internal standard. Standard reaction conditions: $[\mathbf{1a}] = 0.10\text{ M}$, $[\mathbf{2a}] = 0.12\text{ M}$, $[\text{Au}] = 5\text{ mM}$ in 2.0 mL of CDCl_3 under argon at 60°C .

7.26–7.22 (m, 3H); $^{13}\text{C}\{^1\text{H}\}$ NMR (100 MHz, CDCl_3) δ 155.7, 149.4, 137.1, 135.8, 132.1, 131.4, 129.8, 125.0, 124.8, 122.1, 118.7.

Pyrido[1,2-*b*]indazole (**2a**): ^1H NMR (400 MHz, CDCl_3) δ 8.77 (d, $J = 6.8\text{ Hz}$, 1H), 8.08 (t, $J = 6.8\text{ Hz}$, 2H), 7.85 (d, $J = 8.4\text{ Hz}$, 1H), 7.56 (t, $J = 7.6\text{ Hz}$, 1H), 7.32 (t, $J = 7.6\text{ Hz}$, 1H), 7.22 (t, $J = 7.6\text{ Hz}$, 1H), 7.15 (t, $J = 6.8\text{ Hz}$, 1H); $^{13}\text{C}\{^1\text{H}\}$ NMR (100 MHz, CDCl_3) δ 149.6, 135.3, 128.4, 127.9, 121.9, 119.8, 119.7, 117.9, 116.2, 115.5, 115.1.

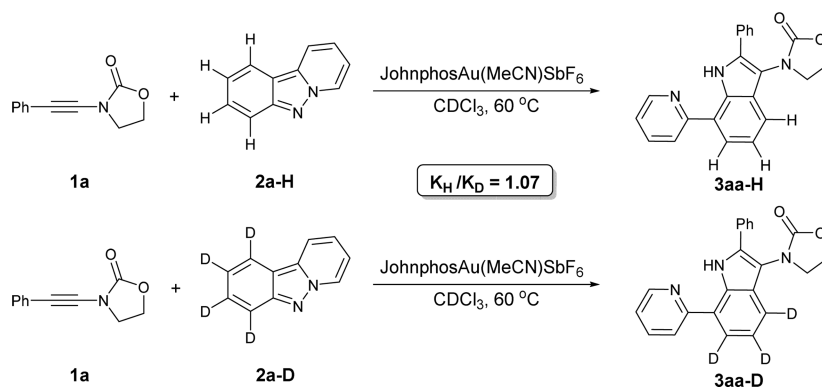
3-Fluoropyrido[1,2-*b*]indazole (**2b**): ^1H NMR (400 MHz, CDCl_3) δ 8.72 (d, $J = 6.8\text{ Hz}$, 1H), 8.02–8.96 (m, 2H), 7.41–7.27 (m, 2H), 7.16–7.12 (m, 1H), 7.00–6.94 (m, 1H); $^{13}\text{C}\{^1\text{H}\}$ NMR (100 MHz, CDCl_3) δ 163.3 (d, $J = 244\text{ Hz}$), 150.2 (d, $J = 13\text{ Hz}$), 135.5, 128.1, 122.9, 121.5 (d, $J = 11\text{ Hz}$), 117.5, 116.0, 112.1, 110.4 (d, $J = 27\text{ Hz}$), 99.4 (d, $J = 24\text{ Hz}$).

3-Chloropyrido[1,2-*b*]indazole (**2c**): ^1H NMR (400 MHz, CDCl_3) δ 8.77 (d, $J = 6.8\text{ Hz}$, 1H), 8.09 (d, $J = 8.8\text{ Hz}$, 1H), 8.00 (d, $J = 8.8\text{ Hz}$, 1H), 7.81 (s, 1H), 7.41 (t, $J = 8.0\text{ Hz}$, 1H), 7.23–7.16 (m, 2H); $^{13}\text{C}\{^1\text{H}\}$ NMR (100 MHz, CDCl_3) δ 150.0, 135.4, 134.3, 128.2, 122.8, 121.0, 120.9, 117.9, 116.6, 114.7, 113.6.

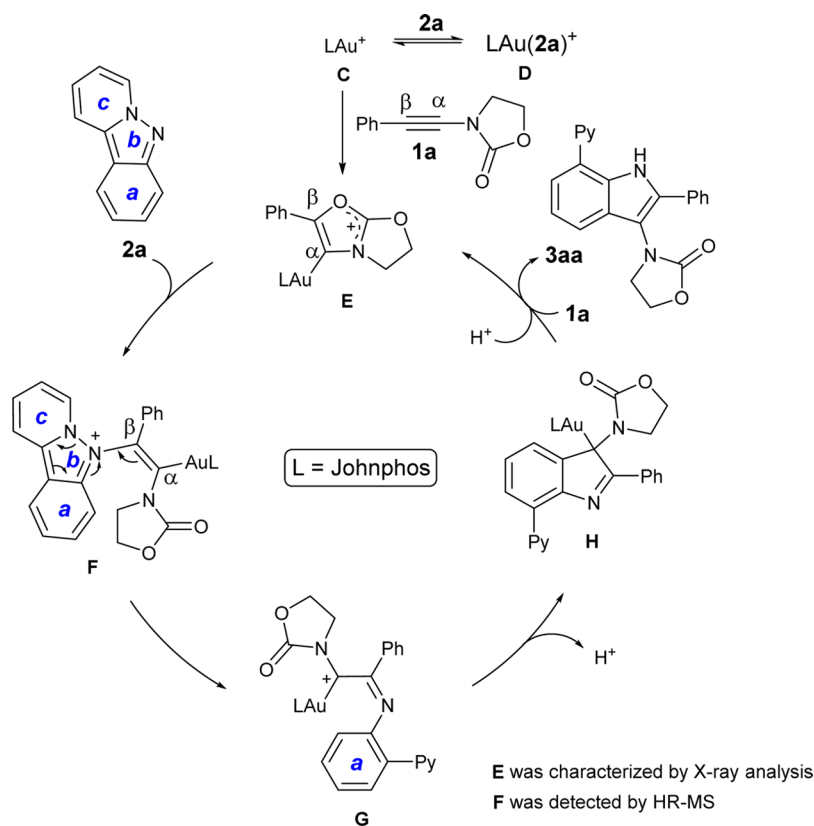
3-Bromopyrido[1,2-*b*]indazole (**2d**): ^1H NMR (400 MHz, CDCl_3) δ 8.72 (d, $J = 6.8\text{ Hz}$, 1H), 8.02 (d, $J = 8.4\text{ Hz}$, 1H), 7.96 (s, 1H), 7.87 (d, $J = 8.4\text{ Hz}$, 1H), 7.36 (t, $J = 7.2\text{ Hz}$, 1H), 7.27–7.17 (m, 2H); $^{13}\text{C}\{^1\text{H}\}$ NMR (100 MHz, CDCl_3) δ 150.3, 135.3, 128.1, 123.1, 122.8, 122.4, 121.1, 117.9, 117.8, 116.6, 113.8.

3-Methylpyrido[1,2-*b*]indazole (**2e**): ^1H NMR (400 MHz, CDCl_3) δ 8.76 (d, $J = 5.6\text{ Hz}$, 1H), 8.07 (d, $J = 8.2\text{ Hz}$, 1H), 7.97 (d, $J = 8.0\text{ Hz}$, 1H), 7.60 (s, 1H), 7.33 (t, $J = 7.2\text{ Hz}$, 1H), 7.16–7.06 (m, 2H),

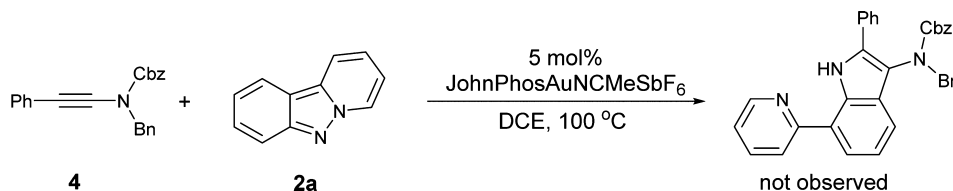
Scheme 3. Kinetic Isotope Effect Experiments



Scheme 4. Mechanistic Rationale



Scheme 5. Reaction of Ynamide 4 with 2a



2.57 (s, 3H); $^{13}\text{C}\{\text{H}\}$ NMR (100 MHz, CDCl_3) δ 150.3, 138.6, 135.3, 127.9, 122.4, 121.9, 119.3, 117.6, 115.7, 114.3, 113.3, 22.4.

3-Methoxyprido[1,2-*b*]indazole (2f): pale yellow solid; yield 244 mg, 61%; mp 102–104 °C; ^1H NMR (400 MHz, CDCl_3) δ 8.72 (d, J = 6.8 Hz, 1H), 8.00 (d, J = 8.8 Hz, 1H), 7.93 (d, J = 8.8 Hz, 1H), 7.33 (t, J = 7.6 Hz, 1H), 7.12–7.07 (m, 2H), 6.90 (d, J = 8.8 Hz, 1H), 3.94 (s, 4H); $^{13}\text{C}\{\text{H}\}$ NMR (100 MHz, CDCl_3) δ 160.7, 151.2, 135.4, 127.9, 122.3, 120.6, 117.1, 114.9, 113.5, 110.0, 93.8, 55.3; IR (KBr) $\tilde{\nu}$ = 1649.0, 1604.5, 1557.7, 1475.2, 1431.5, 1324.5, 1290.3, 1214.9, 1197.9, 1163.3, 801.9, 758.7, 740.6 cm^{-1} ; HRMS (EI) m/z [$\text{M} + \text{H}$] $^+$ calcd for $\text{C}_{12}\text{H}_{11}\text{N}_2\text{O}$ 199.0871, found 199.0866.

Methyl pyrido[1,2-*b*]indazole-3-carboxylate (2g): pale yellow solid; yield 80.0 mg, 15%; mp 180–182 °C; ^1H NMR (400 MHz, CDCl_3) δ 8.83 (d, J = 6.4 Hz, 1H), 8.61 (s, 1H), 8.15 (dd, J = 16.0, 8.4 Hz, 2H), 7.87 (d, J = 8.0 Hz, 1H), 7.42 (t, J = 7.2 Hz, 1H), 7.27 (s, 1H), 4.00 (s, 3H); $^{13}\text{C}\{\text{H}\}$ NMR (100 MHz, CDCl_3) δ 167.5, 149.0, 135.3, 130.1, 128.2, 122.5, 119.9, 119.7, 118.9, 118.6, 117.6, 117.2, 52.3; IR (KBr) $\tilde{\nu}$ = 1715.2, 1432.8, 1366.5, 1303.1, 1219.8, 1144.2, 1081.6, 751.7, 720.6 cm^{-1} ; HRMS (ESI) m/z [$\text{M} + \text{H}$] $^+$ calcd for $\text{C}_{13}\text{H}_{11}\text{N}_2\text{O}_2$ 227.0821, found 227.0815.

3-Phenylprido[1,2-*b*]indazole (2h): pale yellow solid; yield 297 mg, 61%; mp 120–121 °C; ^1H NMR (400 MHz, CDCl_3) δ 8.80 (d, J = 6.4 Hz, 1H), 8.15 (d, J = 7.2 Hz, 2H), 8.03 (s, 1H), 7.75 (d, J = 7.2 Hz, 2H), 7.52–7.36 (m, 5H), 7.21–7.18 (t, J = 6.0 Hz, 1H); $^{13}\text{C}\{\text{H}\}$ NMR (100 MHz, CDCl_3) δ 150.3, 141.7, 141.6, 135.3, 128.8, 128.0, 127.6, 127.4, 122.1, 120.14, 120.07, 117.9, 116.2, 114.4, 113.4;

IR (KBr) $\tilde{\nu}$ = 1644.7, 1596.9, 1533.4, 1507.6, 1421.1, 1362.7, 1339.1, 1212.6, 753.8, 741.3, 722.0 cm^{-1} ; HRMS (ESI) m/z [$\text{M} + \text{H}$] $^+$ calcd for $\text{C}_{17}\text{H}_{13}\text{N}_2$ 245.1079, found 245.1073.

2-Chloropyrido[1,2-*b*]indazole (2i): ^1H NMR (400 MHz, CDCl_3) δ 8.72 (d, J = 6.8 Hz, 1H), 8.00–7.98 (m, 2H), 7.74 (d, J = 9.2 Hz, 1H), 7.46 (dd, J = 9.2, 2.0 Hz, 1H), 7.34–7.30 (m, 1H), 7.18–7.15 (m, 1H); $^{13}\text{C}\{\text{H}\}$ NMR (100 MHz, CDCl_3) δ 147.9, 134.7, 129.3, 128.0, 125.0, 122.3, 118.8, 118.0, 117.0, 116.6, 115.6.

2-Bromopyrido[1,2-*b*]indazole (2j): ^1H NMR (400 MHz, CDCl_3) δ 8.77 (d, J = 6.4 Hz, 1H), 8.23 (s, 1H), 8.08 (d, J = 8.4 Hz, 1H), 7.67 (dd, J = 46, 8.8 Hz, 2H), 7.40 (t, J = 7.2 Hz, 1H), 7.23 (t, J = 6.4 Hz, 1H); $^{13}\text{C}\{\text{H}\}$ NMR (100 MHz, CDCl_3) δ 148.1, 134.6, 131.7, 128.1, 122.5, 122.2, 118.0, 117.3, 116.8, 116.4, 112.5.

1-Methylpyrido[1,2-*b*]indazole (2k): pale yellow oil; yield 96.0 mg, 26%; ^1H NMR (400 MHz, CDCl_3) δ 8.77 (d, J = 6.4 Hz, 1H), 8.13 (d, J = 8.8 Hz, 1H), 7.69 (d, J = 8.8 Hz, 1H), 7.47–7.25 (m, 2H), 7.14–6.96 (m, 2H), 2.80 (s, 3H); $^{13}\text{C}\{\text{H}\}$ NMR (100 MHz, CDCl_3) δ 149.7, 135.6, 132.1, 128.3, 127.8, 121.8, 120.2, 119.5, 115.6, 114.8, 113.0, 20.3; IR (KBr) $\tilde{\nu}$ = 1635.6, 1599.4, 1532.4, 1511.9, 1440.0, 1218.4, 1142.8, 785.7, 740.5, 718.4 cm^{-1} ; HRMS (ESI) m/z [$\text{M} + \text{H}$] $^+$ calcd for $\text{C}_{12}\text{H}_{11}\text{N}_2$ 183.0922, found 183.0917.

1-Chloropyrido[1,2-*b*]indazole (2l): pale yellow solid; yield 132 mg, 32%; mp 90–91 °C; ^1H NMR (400 MHz, CDCl_3) δ 8.76 (d, J = 6.8 Hz, 1H), 8.53 (d, J = 8.8 Hz, 1H), 7.72 (d, J = 8.4 Hz, 1H), 7.46–7.36 (m, 2H), 7.22–7.17 (m, 2H); $^{13}\text{C}\{\text{H}\}$ NMR (100 MHz, CDCl_3) δ 150.5, 135.1, 128.6, 127.9, 127.0, 122.7, 120.1, 119.7, 116.8, 114.1,

J. T. *Chem. Rev.* **2006**, *106*, 2875. (c) Cacchi, S.; Fabrizi, G. *Chem. Rev.* **2005**, *105*, 2873. (d) Cacchi, S.; Fabrizi, G. *Chem. Rev.* **2011**, *111*, PR215. (e) Shiri, M. *Chem. Rev.* **2012**, *112*, 3508.

(21) (a) Black, D. StC.; Bowyer, M. C.; Ivory, A. J.; Jolliffe, K. A.; Kumar, N. *Tetrahedron* **1996**, *52*, 4687. (b) Mudadu, M. S.; Singh, A.; Thummel, R. P. *J. Org. Chem.* **2006**, *71*, 7611.

(22) (a) Wallace, O. B.; Wang, T.; Yeung, K.-S.; Pearce, B. C.; Meanwell, N. A.; Qiu, Z.; Fang, H.; Xue, Q. M.; Yin, Z. US 2003/0069245 A1, 2003. (b) Wang, T.; Zhang, Z.; Meanwell, N. A.; Kadow, J. F.; Yin, Z.; Xue, Q. M. US 2003/0207910 A1, 2003.

(23) Preliminary synthetic applications on the synthesis of BODIPY type dye were explored; for details, see the [Experimental Section](#).

(24) Maulide and co-workers have reported HOTf-mediated reaction of ynamides with organic azides where an intermediate was intercepted by reduction; see: Tona, V.; Ruider, S. A.; Berger, M.; Shaaban, S.; Padmanaban, M.; Xie, L.-G.; González, L.; Maulide, N. *Chem. Sci.* **2016**, *7*, 6032.

(25) (a) García-Cuadrado, D.; Braga, A. A. C.; Maseras, F.; Echavarren, A. M. *J. Am. Chem. Soc.* **2006**, *128*, 1066. (b) García-Cuadrado, D.; de Mendoza, P.; Braga, A. A. C.; Maseras, F.; Echavarren, A. M. *J. Am. Chem. Soc.* **2007**, *129*, 6880. (c) Lafrance, M.; Rowley, C. N.; Woo, T. K.; Fagnou, K. *J. Am. Chem. Soc.* **2006**, *128*, 8754. (d) Lafrance, M.; Fagnou, K. *J. Am. Chem. Soc.* **2006**, *128*, 16496. (e) For a similar acid-catalyzed activation of the analogous alkynylethers in oxygen-transfer reactions, see: Graf, K.; Rühl, C. L.; Rudolph, M.; Rominger, F.; Hashmi, A. S. K. *Angew. Chem., Int. Ed.* **2013**, *52*, 12727.

(26) (a) Wei, L.-L.; Mulder, J. A.; Xiong, H.; Zifcsak, C. A.; Douglas, C. J.; Hsung, R. P. *Tetrahedron* **2001**, *57*, 459. (b) Hamada, T.; Ye, X.; Stahl, S. S. *J. Am. Chem. Soc.* **2008**, *130*, 833. (c) Karad, S. N.; Bhunia, S.; Liu, R.-S. *Angew. Chem., Int. Ed.* **2012**, *51*, 8722. (d) Mukherjee, A.; Dateer, R. B.; Chaudhuri, R.; Bhunia, S.; Karad, S. N.; Liu, R.-S. *J. Am. Chem. Soc.* **2011**, *133*, 15372. (e) Reference 14a..

(27) CCDC 1478721 (3aa), CCDC 1478722 (3ca), CCDC 1478725 (3ah), CCDC 1478727 (JohnphosAu(1a)SbF₆), and CCDC 1478742 (JohnphosAu(2a)SbF₆) contain the supplementary crystallographic data for this paper. These data can be obtained free of charge from the Cambridge Crystallographic Data Centre via www.ccdc.cam.ac.uk/data_request/cif.